Hindawi
International Journal of Aerospace Engineering
Volume 2017, Article ID 2010476, 12 pages
https://doi.org/10.1155/2017/2010476

Research Article

Shock Tube as an Impulsive Application Device

Soumya Ranjan Nanda, Sumit Agarwal, Vinayak Kulkarni, and Niranjan Sahoo

Department of Mechanical Engineering, Indian Institute of Technology Guwahati, Guwahati 781 039, India

Correspondence should be addressed to Niranjan Sahoo; shock@iitg.ernet.in

Received 5 October 2016; Revised 29 January 2017; Accepted 16 February 2017; Published 5 April 2017

Academic Editor: Paul Williams

Current investigations solely focus on application of an impulse facility in diverse area of high-speed aerodynamics and structural mechanics. Shock tube, the fundamental impulse facility, is specially designed and calibrated for present objectives. Force measurement experiments are performed on a hemispherical test model integrated with the stress wave force balance. Similar test model is considered for heat transfer measurements using coaxial thermocouple. Force and heat transfer experiments demonstrated that the strain gauge and thermocouple have lag time of 11.5 and 9 microseconds, respectively. Response time of these sensors in measuring the peak load is also measured successfully using shock tube facility. As an outcome, these sensors are found to be suitable for impulse testing. Lastly, the response of aluminum plates subjected to impulsive loading is analyzed by measuring the in-plane strain produced during deformation. Thus, possibility of forming tests in shock is also confirmed.

1. Introduction

Hypersonic or hypervelocity flows bear complexities due to the thin shear layer, high temperature, and inviscid-viscous interaction. Missiles or launch vehicles encounter this flow regime and hence need special attention in their design phase. A paradigm shift can be noticed in their development over a short span of time due to the impetus of need for space exploration and faster global transportation. Moreover, major challenge ahead the research community lies in accounting impulsive mechanical and thermal loading for safer and cheaper space flights. Hence it is desirable to expose such configurations to the harsh environment as a part of design practice. Flight tests provide one such option, but these tests involve risk and are less cost effective. Therefore, realistic approach, like simulating flight conditions in the laboratories, should be considered for a practical design. Measurement of force for understanding the fuel requirement, heat transfer measurement for designing thermal protection system, and material testing for evaluating the structural strength are the prime motives behind the ground-based testing. In view of this, there is an immediate need to explore for force measurement, heat transfer measurement, and structural health monitoring of associated test configurations in the ground facilities. Various research groups have developed different techniques for the measurement of these design parameters.

Force measurement plays a vital role in design of the aerodynamic vehicles from perspective of its stability and estimation of load on propulsion system. But these experiments, when conducted in impulse facilities (like shock tubes, shock tunnels, or expansion tubes), demand for sophisticated instruments due to very small test flow duration. Typically, two force balance techniques, namely, inertia based [1] and stiffness based [2], have been reported in literature for force measurement. Out of these two techniques, stiffness based balance represents the system more accurately. It relies on measurement of force from strain signal measured either by semiconductor strain gauges or by piezofilm. Simmons [3] and Tuttle et al. [4] considered use of this force balance in free-piston shock tunnel. Another technique of strain measurement with help of polymer piezoelectric film is proposed by Matsumoto et al. [5] where specimens are subjected to uniaxial compressive loading. Calibration of the force balance has been mentioned in these strain based force measurement techniques, but it is also desirable to characterize the strain gauge used for its response time and lag time to justify its applicability in the short duration testing. However, these fundamental requirements are not attended in the open literature.

Prediction of the heat flux becomes very essential parameter to minimize the effect of aerodynamic heating of high-speed vehicles. There are many transient temperature measurement devices available, out of which thin-film and coaxial surface junction thermocouple (CSJT) are very potential candidates to measure the surface heat flux. Rose [6] worked on the development of heat transfer gauge for measuring extremely high heat flux under the quasi-transient conditions occurring in shock tubes. Mohammed et al. and Anderson et al. [7, 8] employed shock tube for carrying out the dynamic calibration and in turn performance assessment of the fast response coaxial thermal sensors. Other researchers also have noticed that coaxial thermocouples are more robust and durable as compared to thin-film sensors when it comes to the application of measuring the heat flux in the harsh environment [9, 10] Moreover, thermal sensors are routinely used in shock tunnels, expansion tubes, free-piston shock tunnel, and gun tunnels [11]. Calibration of the thermal sensor followed by measurement of temperature time history in ground test facilities is the standard procedure for estimation of local heat transfer rate. But this inference largely depends upon the response time and lag time of the sensor due to which special sensors like coaxial thermocouples or thin-film sensors are preferred for these experiments. Hence, it is highly essential to characterize the thermal sensor and test for its robustness before experimentation with the space vehicle model.

Properties like strength, damage tolerance, and crack propagation are the key issues that have to be addressed for the materials generally used for aerospace vehicles. In recent years, shock tube has been used to study the dynamic response of thin metallic plates subjected to varying levels of shock loading [12]. Shock tube, driven with explosives, has also been employed as a device to create a shock loading [13]. Diaphragmless shock tube was considered to study the response of the copper, brass, and aluminum plates [14]. Kumar et al. [15] implemented shock tube as the experimental set-up to study the effect of aluminum panel curvature on blast response where in-plane strain is measured on the back face of the panels. Gray III and Huang [16] investigated the response due to single and repeated shock loading using explosives on aluminum plates. These literature-based findings provide an initiative for application of shock tube in the field of impact testing of materials. Therefore, possibility of simultaneous experimentation for material testing and measurement for impact loading needs to be further explored.

From the open literature, it can be concluded that various researchers have implemented different impulse facilities such as shock tube and shock tunnel for measurement of force, heat transfer, or material testing. All these ground test facilities are evolved from shock tube fundamentals. Besides, shock tube testing is cheaper and effective when it is concerned with possibility of usage of a sensor, its robustness testing or characterization. Jagadeesh [17] had proved the usefulness of this impulse facility for industrial applications. Therefore, shock tube can be considered as the first experimental set-up to test sensors in the ambience involving highly transient compressible flow. In view of above facts, an attempt has been made to access the potential use of shock tube for determining fundamental constants of the sensors used in force and heat transfer measurements. These characteristic constants include "response time and lag time" of the sensors. Possibility of material testing against the impulse loading and associated measurement is also planned herein. With successful demonstration, such types of use of shock tube would become an integral part of sensor development. Hence, an initiative is taken to assess the usefulness of the shock tube in sensor and material testing. As a part of this drive, a shock tube is designed in-house, fabricated and calibrated successfully and, then, employed as an aerotest facility. In this phase, numerical simulations are also performed to get detailed insight of shock tube flow. Three major experiments are conducted in the shock tube, which include force measurement using strain gauge, heat transfer rate measurement using thermocouple, and deformation testing of aluminum sheets. The details of shock tube and associated experiments and the numerical simulations are explained in the subsequent sections.

2. Computational Investigation

2.1. Shock Tube Facility. The shock tube facility at "Indian Institute of Technology Guwahati (IITG), India", is made out of stainless steel material and has 2 m long driver section and 5 m long driven section. These sections are assembled using 1 m long tubes of inner diameter 55 mm and thickness 12 mm. For present studies, aluminum diaphragm of 1.2 mm thickness with V-grooves is considered to separate two sections of the shock tube. The driver section is equipped with high pressure digital pressure gauges, whereas vacuum pressure in the driven section is measured by Pirani gauge. Two pressure transducers (PCB make) have also been flush-mounted to the inner surface of the driven section for measuring the pressure jump in the presence of incident and reflected shock waves. Further, usage of these pressure signals is helpful in deducing their Mach numbers. The entire shock tube assembly with associated instrumentation is illustrated in Figure 1. In the most of the present studies, driver gas is chosen to be helium having temperature of 298 K and pressure of 19.85 bar, while air is maintained at 298 K and 0.18 bar as the driven gas.

2.2. Numerical Simulation. Before execution of the experiments in the actual test facility, numerical simulation of the same is necessary as it provides a clear visualization and better insight of the flow inside the domain. Also it offers essential information about magnitude of signals to be acquired and associated data acquisition settings. Hence, numerical simulation of complete shock tube is carried out by usage of the commercial CFD solver (ANSYS FLUENT 14.5), where governing equations of continuity, momentum, and energy are solved using finite volume approach. In order to incorporate the effect of different driver and driven gas species, transport equation is also solved herein. The computational domain along with its associated initial and boundary conditions is shown in Figure 2.

As the axisymmetric approach is sufficient to render an accurate description of the real flow configuration, so the shock tube is modeled as an axisymmetric body. Meshing of the flow domain is initially done by mapped facing method

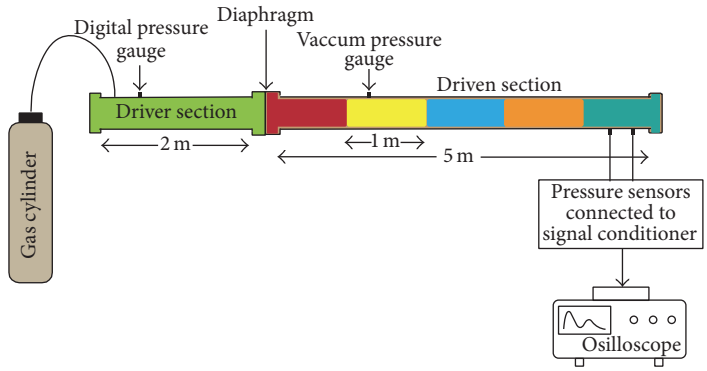

Figure 1: Shock tube facility present at IIT Guwahati.

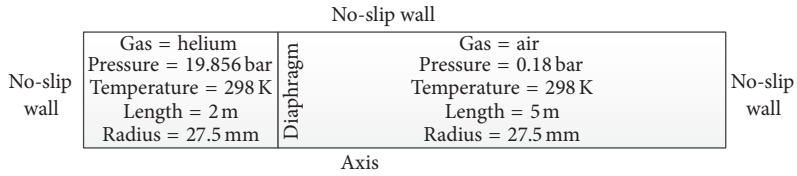

Figure 2: Computational domain and its boundary conditions.

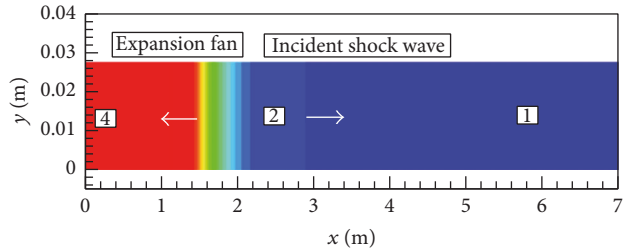

Figure 3: Pressure distribution after diagram rupture.

which is then modified by uniform quad method. Density based implicit solver with four-stage Runge-Kutta scheme has been chosen for transient analysis of the flow field. For the current numerical simulation, "advection upstream splitting method (AUSM)" flux vector splitting scheme has been adopted to compute the convective fluxes. User-defined function (UDF) has been incorporated in the present situation to initialize the computational domain into two different sections, namely, driver and driven sections. Bursting of the diaphragm is not the prime concern, so the diaphragm is assumed to be ruptured instantly at time $t = 0$. Initial conditions set in the computational domain are as given in Figure 2. This figure also describes the boundary conditions for the present problem. Simulations are performed for different time steps and mesh sizes so as to arrive at an optimum combination. Finally, the chosen mesh (320000 nodes) and time step have fetched the results, which are independent of the mesh size and time step with adequate resolution of the flow field. Pressure contours after 0.9 ms of the rupturing of the diaphragm are shown in Figure 3. It gives clear visualization of a right-running incident shock wave and a left-running expansion fan. The incident shock hits the end wall and reflects back creating high temperature and pressure zone behind it, which is evident in Figure 4.

Initial conditions of the shock tube are also used to obtain the x-t diagram using the tool of Wisconsin Shock Tube Laboratory [8]. Space-time details of different waves can be obtained using such x-t diagram. Essentially, it is an exact Riemann solver which employs a 2nd-order Muscl-Hancock method in finite volume formulation. Result of these simulations in the form of x-t diagram is shown in Figure 5. This figure clearly shows that the present operating conditions lead to tailored mode operation of the shock tube. Further, different wave speeds and the pressure change across the wave can also be evaluated using the slope of the x-t diagram.

It has been observed, from CFD simulations, that the primary shock wave requires 4.4 ms to reach the end wall. Similarly, x-t diagram suggests that the shock would take 3.96 ms to reach the driven section end after bursting of the diaphragm. Further, as both primary and reflected shocks are the concerned factors during experiments, so the parameter

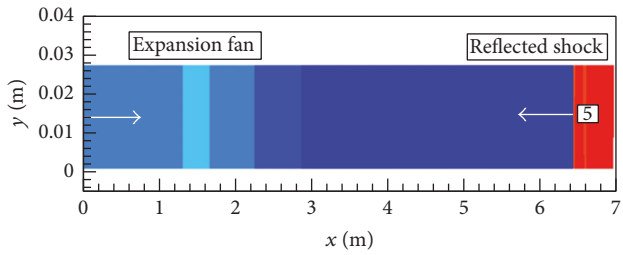

Figure 4: Pressure distribution after reflection from end wall.

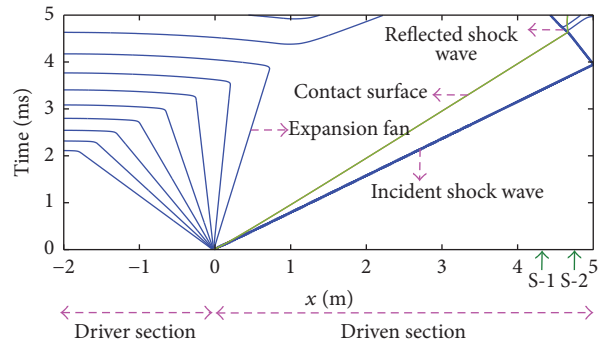

Figure 5: Representation of shock tube operating conditions in x-t diagram.

jump across these shocks is the critical information acquired as an outcome of computational efforts. Pressure and temperature expected behind the primary shock are 3.23 bar and 1029 K from the CFD simulation. Mach number of predicted by this simulation for primary shock is noted to be 3.6, while the induced mass motion behind this shock has Mach number of 1.49. Similarly, primary shock Mach number and pressure behind it, predicted from exact Riemann solver, are 3.65 and 2.75 bar, respectively. These results are found to be useful for designing and planning of the proposed experiments.

3. Calibration of Shock Tube

For the calibration experiments, driver and driven sections of the shock tube are separated by aluminum diaphragm. As considered for simulation, helium is chosen to be the driver gas and air is considered as the driven gas. In one of the experiments, initial pressure of the driven section is maintained at 0.18 bar, whereas pressure inside the driver section is increased till it reaches rupture pressure of the diaphragm. Before the actual experiments, driven section of the shock tube is evacuated to the known low pressure. Then driver gas is supplied in the driver section from the standard pressure cylinders till the diaphragm ruptures. The driver section pressure is measured to be 19.85 bar with an uncertainty of ±0.02%. Sudden rupture of the diaphragm resulted in a shock wave that propagates into the driven section which further induces a mass motion in the driven gas. This primary shock subsequently reflects from shock tube end wall. Typical pressure signal obtained during experiment from two pressure transducers is shown in Figure 6. Measured pressures can be used to evaluate the pressure ratios. Here, shock speed and onwards shock Mach number are calculated from the distance between both pressure transducers and time taken by the shock wave to travel the same distance. Calibration experiments of the shock tube showed reasonably good agreement with the theoretical and simulation based predictions. Experimentally measured pressure ratio across the primary shock is 16.73, while the same predicted from the shock tube theory is 15.59. Estimation of the pressure ratio across the primary shock from CFD simulations is 17.89, while the same ratio is predicted as 15.27 using exact Riemann solver. Similarly, experimental, theoretical, CFD, and exact Riemann solver based primary shock Mach numbers for the same shock tube driving conditions are 3.49, 3.68, 3.6, and 3.65, respectively. These results show that the experimental shock Mach number deviates 5.1% from the theoretical value, 2.1% from the CFD simulations, and 4.6% from estimation of exact Riemann solver. Along with the encouraging comparison, successful opening of metal diaphragm has been noticed as an outcome of these calibration experiments. Hence, these operating conditions are considered for experiments with force and heat transfer measurement sensors.

4. Applications of Shock Tube

4.1. Impulsive Force Measurement. Experimentation in impulse facilities needs sophisticated instrumentation since these facilities are characterized by small test duration (~ of 10 microseconds to 1 millisecond). Like other measurements, force measurement needs special attention due to difficulty in attaining steady state between the mounting system and test configuration. Therefore, shock tube testing is a viable

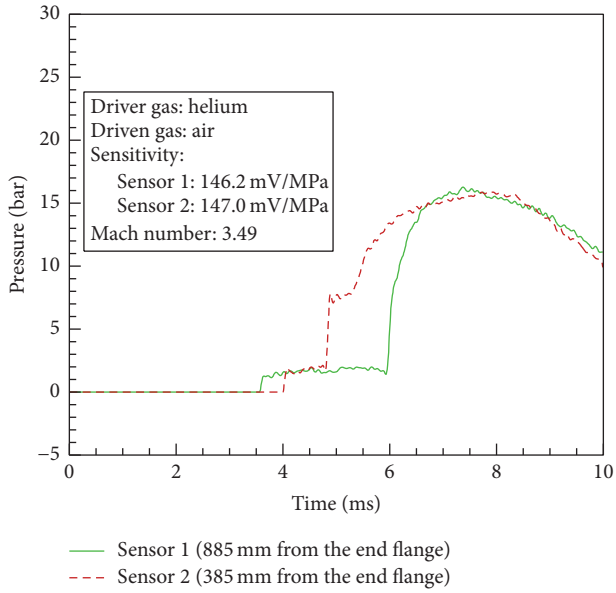

Figure 6: Pressure signal acquired in the shock tube using helium as the driver gas.

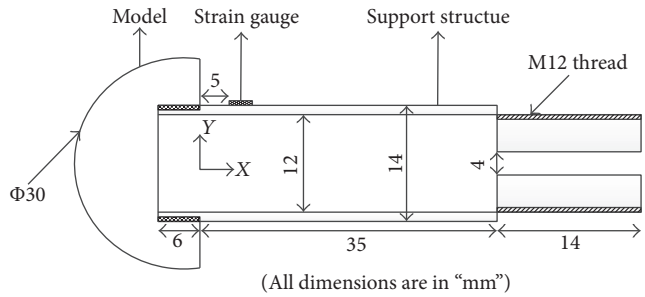

Figure 7: Schematic drawing of the hemispherical model.

alternative to assess the possibility of force measurement using a force balance since the test model experiences highly transient flow in this test facility.

The hemispherical test model (15 mm radius) made out of aluminum and attached with a brass stress bar (14 mm diameter and thickness 1 mm) is considered to be the test model for force measurement purpose (Figure 7). This model is equipped with stress wave force balance for the output response measurement in terms of strain. Here, strain is measured with the help of encapsulated semiconductor strain gauge having resistance 350 Ω and gauge factor 130. This strain gauge is mounted at a distance of 5 mm from the rear end of the hemispherical model. Strain gauge is further connected to Wheatstone bridge circuit for measuring the resistance change. The output of the Wheatstone bridge is of the order of few microvolts, while a voltage amplifier of gain factor 500 is used for amplifying the voltage response. Further, the output terminal of the amplifier is connected to the oscilloscope through BNC connecters for recording the signal during experiment.

The mentioned model in Figure 7 equipped with strain gauge is dynamically calibrated before testing in shock tube. During this dynamic calibration, model is fixed in a bench vice and impulse force is applied using the impulse hammer. Recorded strain signals and corresponding applied force time histories are shown in Figures 8 and 9, respectively. One such strain signal and corresponding force impulse signal are considered to obtain the system response function. Later, this response function and other strain signal from calibration experiment are employed to recover the applied force using MATLAB based FFT program. Encouraging recovery of force signals is evident in Figure 9.

Experiments are then carried out on the hemispherical test model with stress bar mounted with strain gauge in the shock tube. Mounting of the strain gauge is maintained at the same location as it was kept during the calibration experiments. For these experiments, model and stress bar assembly is fixed in the end flange located at the driven section end of the shock tube. Force measurement experiments are then conducted for the same initial conditions of shock tube calibration tests. Shock tube pressure signals are also recorded along with the strain signal in these experiments. Various sets of experiments have been carried out to verify the consistency and repeatability of measurement.

Strain time history along with the pressure signal of second pressure transducer is shown in Figure 10. Here, strain

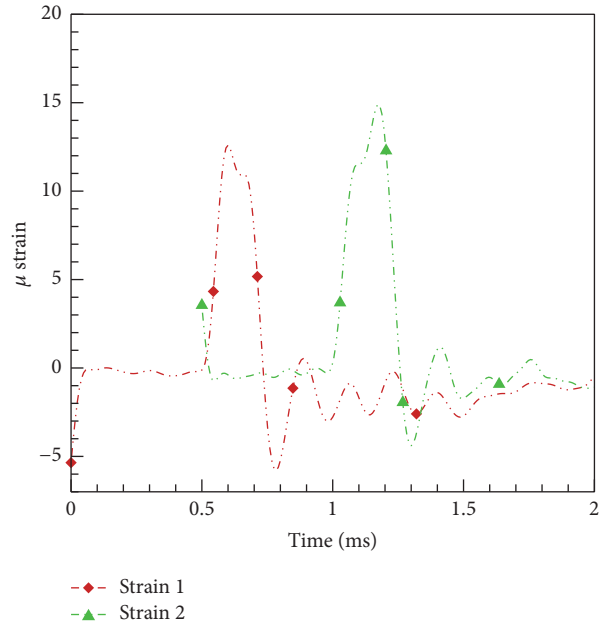

Figure 8: Strain signals recorded in two calibration tests.

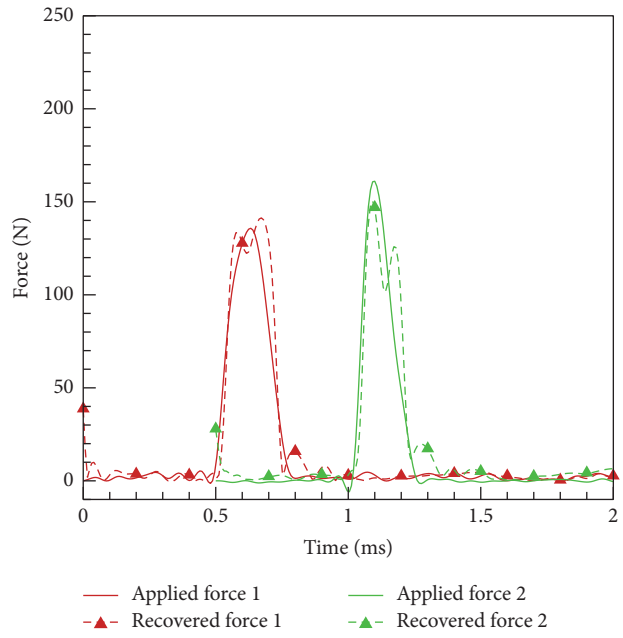

Figure 9: Applied and recovered force signals of two calibration tests.

signal has been filtered using "Butterworth low pass filter" having cut-off frequency of 12.5 kHz. Lag time of the strain gauge can be estimated by interpreting these signals. For this experimental condition, speed of the shock wave is 1108 m/s, so the theoretical time required for the shock wave to travel between second pressure transducer and the test model is 316.08 microseconds. The time difference between response of pressure transducer and strain gauge (Figure 10) is 327.59 microseconds. Thus, the lag time of the presently used strain gauge is calculated as, 11.51 microseconds. Such a small lag time of this sensor makes it perfectly applicable for force measurements in short duration impulse facilities. Further, this strain response is used to predict the drag force acting on the model by using deconvolution technique as illustrated in Figure 10. Response time of the sensor for force measurement is depicted in this figure (258 microseconds). It is evident that force measurement and strain gauge characterization is very much possible using shock tube. Thus, present investigations are found to be useful for implementation of shock tube in the area of force measurement on aerodynamic bodies.

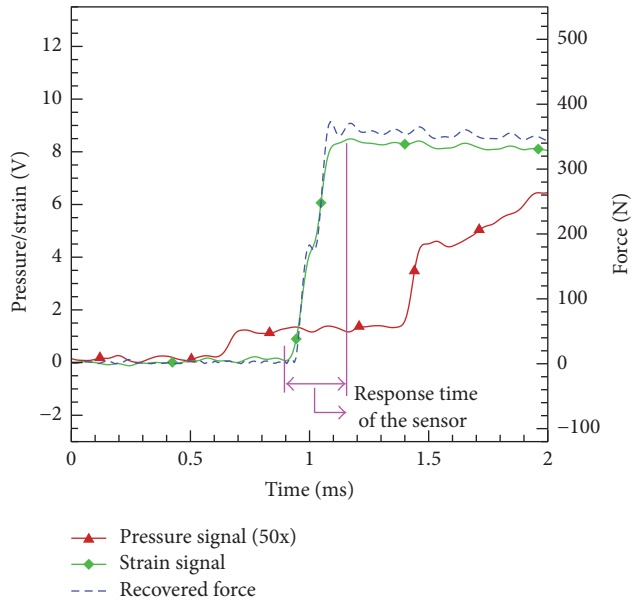

Figure 10: Experimentally obtained pressure and strain signal along with associated recovered force.

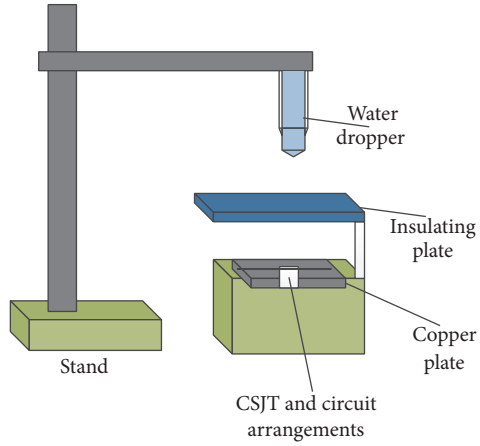

Figure 11: Schematic of the experimental set-up for estimation of thermal product.

4.2. Heat Flux Measurement. An attempt has been made to obtain specifications of thermal sensor and to measure the heat flux in the highly transient environment of the shock tube in order to review the application of shock tube as heat flux measurement device. Attainment of thermal equilibrium between the test object and the fluid flow is not possible due to small test duration. Therefore, the rate of temperature rise is invariantly measured for heat transfer rate prediction. On similar lines, heat transfer measurement experiments are carried out using a hemispherical aluminum model of radius 10 mm. An E-type (chromel-constantan) coaxial thermal sensor having diameter of 3.25 mm has been considered to measure the heat flux. This coaxial thermal sensor always gives the signal in the form of voltage as it works on the principle of Seebeck effect. Provision is made at the stagnation point of the model for mounting this thermocouple. The coaxial surface junction thermocouple (CSJT) has a surface junction where one element is swaged over the other element with a layer of electrical insulation in between them. The junction of the sensor is formed by slightly abrading one material over the other in turn creating plastic deformation of two materials. The sensor has a sensitivity of 58.96 μV/°C, which is obtained from oil bath calibration of the sensor. The fabrication and calibration techniques are considered from [18].

An in-house experimental set-up is employed to measure the thermal product of the E-type coaxial surface junction thermocouple. This measurement procedure is generally termed as "water-droplet" technique for thermal product estimation. Schematic of the set-up is as shown in Figure 11. This arrangement is comprised of copper plate equipped with surface mounted E-type thermocouple. Water drop (at temperature of 26°C) from the dropper is allowed to fall on the thermocouple from a fixed location. Here, distance

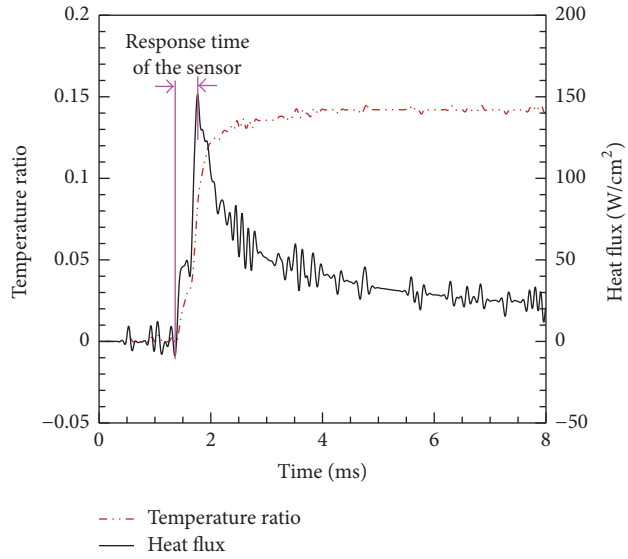

Figure 12: Temperature and corresponding heat flux signal for a water drop test.

between plate and the dropper is maintained using height adjustor. During the experiment, copper plate is heated using electric heater and its temperature is maintained at 50°C. An insulating plate is kept between the copper plate and the dropper to avoid the thermal influence of plate on the water drop.

It has been noticed that the water drop impact does not affect the surface junction of the thermocouple. Temperature time history, obtained during the experiment, is as shown in Figure 12, and (1) is used to compute the thermal product of the thermocouple:

$$\frac{T - T_s}{T_s - T_w} = \frac{\beta_w}{\beta_w + \beta}. \tag{1}$$

Here, required thermal product of water, β_w (=1643 J m^{-2} K^{-1} s$^{-0.5}$), is taken from the available literature [7, 8]. As an outcome of this experiment, presently, using E-type thermocouple is seen to have thermal product of 9493 J·m^{-2}·K^{-1}·s$^{-0.5}$. Generally, for such short duration time scale applications, heat transfer rates can be recovered from the transient temperature data, through the use of appropriate modeling of (2) with assumption of one-dimensional heat conduction [19, 20]:

$$q_L(t) = \frac{\beta}{\sqrt{\pi}}\left[\frac{T(t)}{\sqrt{t}} + \frac{1}{2}\int_0^t \frac{T(t) - T(\tau)}{(t-\tau)}\right]; \qquad \beta = \sqrt{\rho c k}. \tag{2}$$

Furthermore, as the thermal penetration depth during the experimental run times is small compared to the linear dimension of the thermal sensor, the system can be modeled by considering unsteady, linear conduction of heat in a one-dimensional semi-infinite solid [20]. In order to use (2), it is desirable to have a closed form solution of transient temperature data obtained from the captured experimental signals [10]. There are many discretization techniques available; but, for the present study, a polynomial based cubic-spline discretization technique is utilized to discretize the obtained temperature data (see (3) and (4)):

$$\begin{aligned}\{q_L(t)\}_{\text{spline}} = \Bigg[& 2\sqrt{\frac{\rho_2 c_2 k_2}{\pi}} \sum_{i=1}^{M-1} \left\{ V_i \left(P_i^{1/2} - R_i^{1/2}\right) \right. \\ & \left. - \frac{W_i}{3}\left(P_i^{3/2} - R_i^{3/2}\right) + \frac{a_{4,i}}{10}\left(P_i^{5/2} - R_i^{5/2}\right) \right\} \\ & + 2\sqrt{\frac{\rho_2 c_2 k_2}{\pi}} \left(V_M - P_M^{1/2} - \frac{W_M}{3} P_M^{3/2} + \frac{a_{4,i}}{10} P_M^{5/2}\right) \Bigg] \\ & \cdot \sqrt{S_t},\end{aligned} \tag{3}$$

where

$$\begin{aligned} P_i &= \tau_{M+1} - \tau_i; \\ R_i &= \tau_{M+1} - \tau_{1+i}; \\ F_i &= a_{1,i} + a_{2,i} P_i + \frac{a_{3,i}}{2} P_i^2 + \frac{a_{4,i}}{6} P_i^3; \\ V_i &= \frac{dF_i}{d\tau_{M+1}}; \\ W_i &= \frac{d^2 F_i}{d\tau_{M+1}^2}; \\ S_t &= \text{time scaling factor.} \end{aligned} \tag{4}$$

The reduced heat flux signal processed with above technique from the temperature data is presented in Figure 12. This figure gives the information about response time of the sensor. It is evident here that the response time of the E-type CSJT in recovering peak heat flux is 375 microseconds.

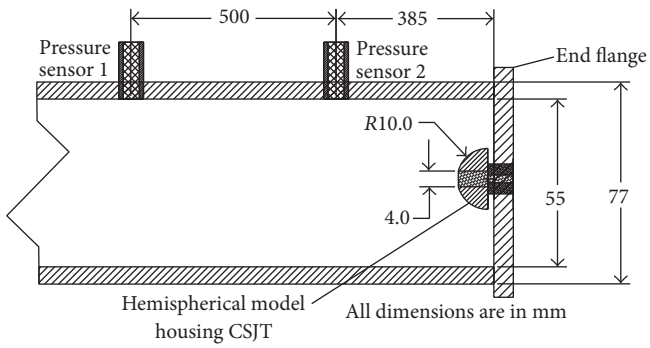

FIGURE 13: Schematic of the end-section of the shock tube showing the mounting of coaxial thermocouple on the hemispherical model at the end flange.

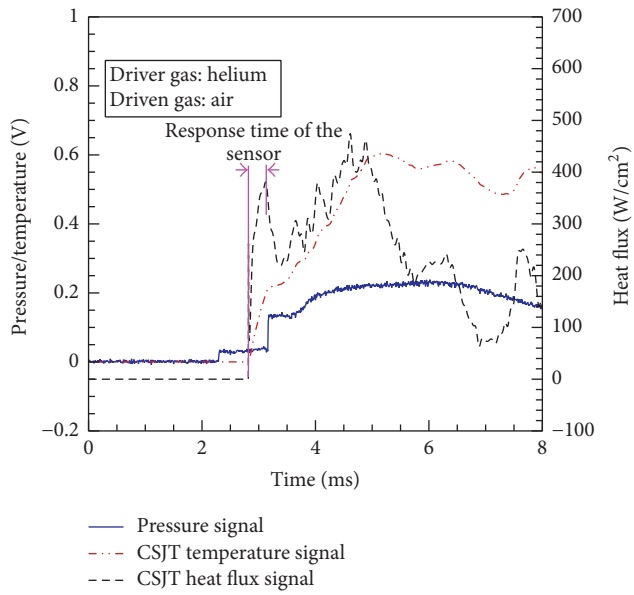

FIGURE 14: Temperature and heat flux variation for the spherical test model in shock tube test.

A test model integrated with thermocouple, flush-mounted at stagnation point, is then considered for measurement of stagnation heat flux in the shock tube. This spherical model of radius 10 mm is mounted on the end flange of the shock tube as shown in Figure 13. Same experimental settings are preferred as those used in force measurement experiments. The experimental temperature signal along with the pressure signal from second pressure transducer and heat flux histories (processed from temperature data by using (2)) is compared in Figure 14. Response time of the thermocouple can be estimated using the time varying heat transfer rate. These shock tube experiments depict that the response time of the E-type CSJT in recovering peak heat flux is 307 microseconds.

Separate experiment is conducted for lag time measurement of the in-house developed E-type CSJT. In this experiment, one coaxial thermocouple is flush-mounted in the end flange of the shock tube. Nitrogen is used here as driver gas to burst the same diaphragm of 1.2 mm thickness. Air pressure in the driven section is maintained as 0.18 bar. As an outcome of this experiment, temperature time history along with the pressure signal from second pressure transducer is shown in Figure 15. Lag time was calculated from these signals with known shock speed and it is found to be 9 microseconds for the in-house E-type CSJT. Fast reaction for the applied heat load makes this thermal sensor perfectly suitable for measurement in impulse facilities. Heat transfer rate is also estimated from the temperature time history as predicted in earlier cases (Figure 15). Response time for the peak heat flux is noted here as 352 microseconds. Thus, it is evident here that the shock tube can be used for measurement of lag time and response time of the thermocouple. Present efforts also portray that the E-type coaxial thermocouples have sufficiently low lag time and rise time in the range of 300–400 microseconds for predicting the peak heat flux.

4.3. Forming Response Study. Material strength and deformation characteristics under high pressure and temperature environment play a crucial role in designing aerodynamic

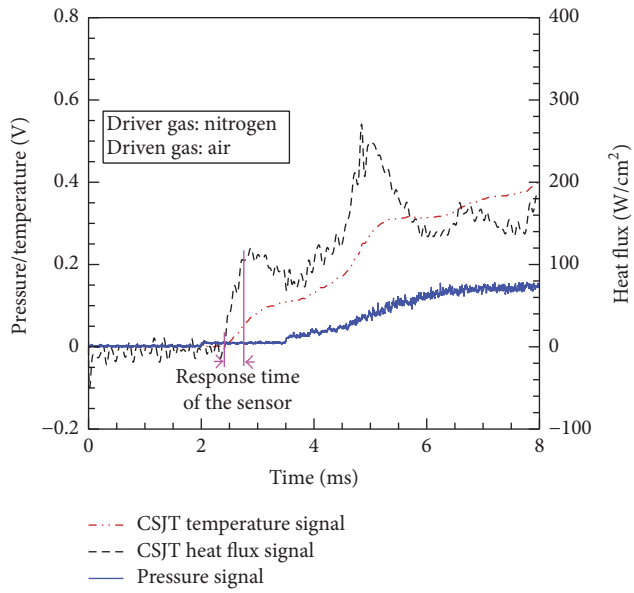

Figure 15: Temperature and heat flux variation for the end flange mounting of shock tube.

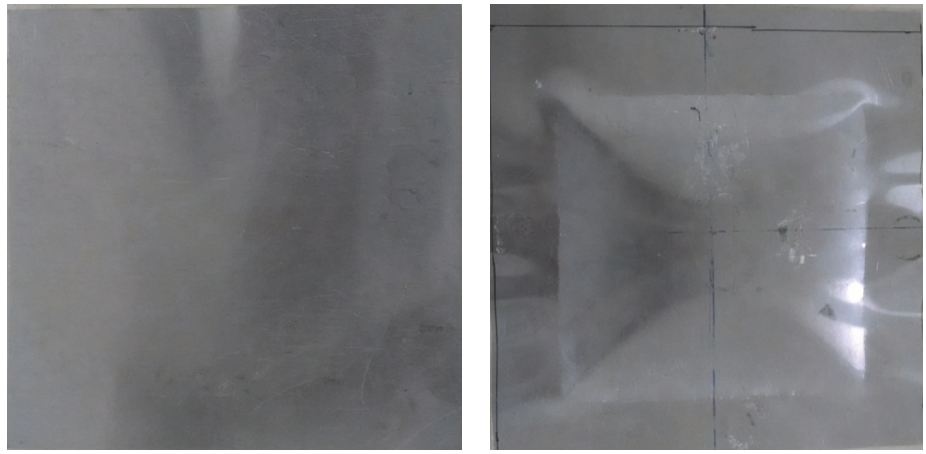

(a) (b)

Figure 16: (a) Initial test specimen. (b) Deformed shape due to shock loading.

vehicles. Generic aerospace applications make usage of aluminum and its alloys for fabrication purpose. Hence, to check the sustainability and stability of the materials subjected to impulse loading, preliminary forming study has been done. Shock tube is employed as a device for generation of high pressure impact loading. Same shock tube but with 2 m driver section and 2 m driven section is employed for the current investigation. Mylar sheets of 1 mm thickness have been chosen instead of metal diaphragm for the preliminary forming tests. The test specimen is considered as a flat plate of aluminum having 0.5 mm thickness. This plate is clamped at the end of the driven section during the experiment. The maximum in-plane strain in the specimen during experiment is measured with the help of semiconductor strain gauge having resistance of 7500 Ω and gauge factor 175. This strain gauge is glued at the centre of back surface of the sample along the horizontal axis. It is further connected to Wheatstone bridge circuit and voltage amplifier as a part of the data acquisition network. During the experiments, driven section is maintained at atmospheric pressure, whereas the driver section pressure is increased till rupture of the Mylar sheet. The bursting pressure is noticed to be 20 bar with an uncertainty of ±9%. From the pressure signal obtained through pressure transducers, it is evident that maximum incident pressure on to the plate is 2.73 bar. In fact, it is the pressure behind the reflected shock. Aluminum specimen is found to be deformed due to application of this impulse force. Initial and deformed plates are shown in Figure 16. The trend of deformation of the plate has reasonably good match with Kumar et al. [15]. Typical strain and pressure signal obtained has been shown in Figure 17. An instant rise in strain response can be seen from the figure as realised practically. Thus,

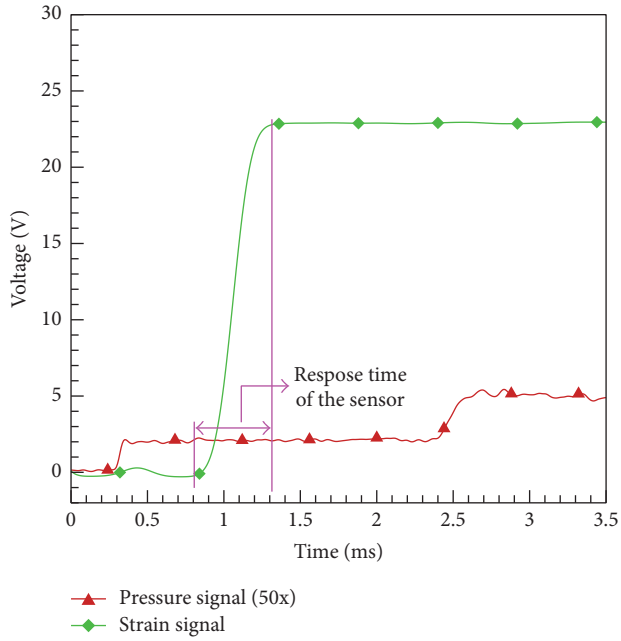

Figure 17: Obtained pressure and strain response during forming experiment.

present experiments demonstrate the use of shock tube for material response or forming studies as well.

5. Conclusion

A shock tube is successfully fabricated and calibrated and is effectively considered to demonstrate multiple applications. At the first phase, insight of the shock tube flow physics is earned through CFD simulations. Initially, this sophisticated experimental set-up is considered for force measurement experiments on a hemispherical model equipped with a high gauge factor strain gauge. From the output response, drag force is predicted using deconvolution technique through the system response function obtained during dynamic calibration. In this experiment, lag time and response time of the strain gauge are noticed to be 11.5 and 258 microseconds, respectively. Similarly, transient temperature change is recorded using a calibrated thermocouple for a hemispherical test configuration subjected to the shock tube flow conditions. Transient temperature time history has also been measured for the end flange mounting of the thermocouple in the shock tube. Further, using cubic-spline discretization method, stagnation point heat flux is calculated. These experiments portrayed that the E-type CSJT has lag time of 9 microseconds and rise time in the range of 300–400 microseconds. Since, in both the experiments, sensors could sustain the impulsive mechanical and heat load while recording the signal, these experiments in the shock tube showed that it is indeed possible to test the sensors for their characterization and robustness. Further experiments are also performed successfully on an aluminum plate subjected to impulse loading in shock tube for assessing its formability. During these experiments, in-plane strain is effectively measured using strain gauge. Thus, current study provides an ample scope of shock tube application in regard to force and heat flux measurement as well as structural behavior study for impulse loading.

Conflicts of Interest

The authors declare that there are no conflicts of interest regarding the publication of this paper.

Acknowledgments

The financial support received from "Aeronautical Research and Development Board (AR & DB)," and "Gas Turbine Materials and Processes (GTMAP)," Government of India (New Delhi), is highly acknowledged.

References

[1] N. Sahoo, D. R. Mahapatra, G. Jagadeesh, S. Gopalakrishnan, and K. P. J. Reddy, "Design and analysis of a flat accelerometer-based force balance system for shock tunnel testing," *Measurement*, vol. 40, no. 1, pp. 93–106, 2007.

[2] S. R. Sanderson and J. M. Simmons, "Drag balance for hypervelocity impulse facilities," *AIAA journal*, vol. 29, no. 12, pp. 2185–2191, 1991.

[3] J. M. Simmons, "Measurement techniques in high-enthalpy hypersonic facilities," *Experimental Thermal and Fluid Science*, vol. 10, no. 4, pp. 454–469, 1995.

[4] S. L. Tuttle, D. J. Mee, and J. M. Simmons, "Drag measurements at Mach 5 using a stress wave force balance," *Experiments in Fluids*, vol. 19, no. 5, pp. 336–341, 1995.

[5] E. Matsumoto, S. Biwa, K. Katsumi, Y. Omoto, K. Iguchi, and T. Shibata, "Surface strain sensing with polymer piezoelectric film," *NDT & E International*, vol. 37, no. 1, pp. 57–64, 2004.

[6] P. H. Rose, "Development of the calorimeter heat transfer gauge for use in shock tubes," *Review of Scientific Instruments*, vol. 29, no. 7, pp. 557–564, 1958.

[7] H. A. Mohammed, H. Salleh, and M. Z. Yusoff, "Dynamic calibration and performance of reliable and fast-response coaxial temperature probes in a shock tube facility," *Experimental Heat Transfer*, vol. 24, no. 2, pp. 109–132, 2011.

[8] M. H. Anderson, B. P. Puranik, J. G. Oakley, P. W. Brooks, and R. Bonazza, "Shock tube investigation of hydrodynamic issues related to inertial confinement fusion," *Shock Waves*, vol. 10, no. 5, pp. 377–387, 2000.

[9] R. Kumar, N. Sahoo, and V. Kulkarni, "Conduction based calibration of handmade platinum thin film heat transfer gauges for transient measurements," *International Journal of Heat and Mass Transfer*, vol. 55, no. 9-10, pp. 2707–2713, 2012.

[10] R. Kumar and N. Sahoo, "Dynamic calibration of a Coaxial thermocouples for short duration transient measurements," *Journal of Heat Transfer*, vol. 135, no. 12, Article ID 124502, 2013.

[11] K. Hariprakasham, M. D. Kumar, and T. Mukesh, "To develop a coaxial thermocouple sensor for temperature measurement in shock tube," *International Journal of Advanced Information Science and Technology*, vol. 27, pp. 2319–2682, 2014.

[12] N. Ray, G. Jagadeesh, and S. Suwas, "Response of shock wave deformation in AA5086 aluminum alloy," *Materials Science and Engineering A*, vol. 622, pp. 219–227, 2015.

[13] M. A. Louar, B. Belkassem, H. Ousji et al., "Explosive driven shock tube loading of aluminium plates: experimental study," *International Journal of Impact Engineering*, vol. 86, pp. 111–123, 2015.

[14] S. R. Nagaraja, J. K. Prasad, and G. Jagadeesh, "Theoretical-experimental study of shock wave-assisted metal forming process using a diaphragmless shock tube," *Proceedings of the Institution of Mechanical Engineers, Part G: Journal of Aerospace Engineering*, vol. 226, no. 12, pp. 1534–1543, 2012.

[15] P. Kumar, J. LeBlanc, D. S. Stargel, and A. Shukla, "Effect of plate curvature on blast response of aluminum panels," *International Journal of Impact Engineering*, vol. 46, pp. 74–85, 2012.

[16] G. T. Gray III and J. C. Huang, "Influence of repeated shock loading on the substructure evolution of 99.99 wt.% aluminum," *Materials Science and Engineering: A*, vol. 145, no. 1, pp. 21–35, 1991.

[17] G. Jagadeesh, "Industrial applications of shock waves," *Proceedings of the Institution of Mechanical Engineers, Part G: Journal of Aerospace Engineering*, vol. 222, no. 5, pp. 575–583, 2008.

[18] S. Agarwal, N. Sahoo, and R. K. Singh, "Experimental techniques for thermal product determination of coaxial surface junction thermocouples during short duration transient measurements," *International Journal of Heat and Mass Transfer*, vol. 103, pp. 327–335, 2016.

[19] D. L. Schultz and T. V. Jones, "Heat transfer measurements in short duration hypersonic facilities," Tech. Rep. AGARD-AG-165, 1973.

[20] J. Taler, "Theory of transient experimental techniques for surface heat transfer," *International Journal of Heat and Mass Transfer*, vol. 39, no. 17, pp. 3733–3748, 1996.